# Design and fabrication of a dual-element off-axis near-eye optical magnifier

**Ozan Cakmakci* and Jannick Rolland**

*CREOL, College of Optics & Photonics, University of Central Florida, Orlando, Florida, 32816, USA*
**Corresponding author: ozan.cakmakci@gmail.com*

Received December 8, 2006; revised March 6, 2007; accepted March 8, 2007;
posted March 15, 2007 (Doc. ID 77917); published April 24, 2007

The key contribution is the design, analysis, and fabrication of a dual-element off-axis magnifier to improve the state of the art in catadioptric magnifiers. The catadioptric magnifier is composed of a free-form mirror and a lens with a diffractive optical element. A monocular magnifier was prototyped, to our knowledge for the first time, with the specifications of an 8 mm exit pupil, 20° diagonal full field of view, 15 mm eye clearance, 1.5 arcmin resolution, and operating in the photopic visual regime. 

*OCIS codes:* 220.2740, 220.4830, 050.1970.

The design of compact magnifiers is important in applications such as mobile information displays [1]. The applications of the design presented in this Letter are personal information management, reading or writing notes and e-mails, watching multimedia content, and visual overlays assisting the task at hand. The optical magnifier presented in this Letter is intended to be coupled monocularly with the human visual system under photopic conditions.

A single spherical surface configured in an off-axis manner was proposed by Bettinger [2]. Holographic optical elements (HOEs) were applied to the eyeglass-based display problem. A head-worn display with a 3 mm exit pupil and a $27° \times 10°$ field of view, operating at the single wavelength of 532 nm, was designed based on a HOE and was fabricated [3]. However, full color (red, green, and blue) displays based on HOEs are currently a challenging research problem. A second alternative in the design of compact optical magnifiers is to use a laser source and to scan the image onto the retina. However, as can be explained by the Lagrange invariant, the exit pupil of such a scanner is small, and pupil expansion mechanisms are required. Pupil expanders add additional complexity and size to the whole system, which deviates from the goal of compact magnifiers with high image quality.

Our approach is to consider one or two element magnifier designs and explore their performance and field of view limits. The design form presented in this Letter is an off-axis magnifier that folds the optical axis around a human head while providing the necessary clearances. The symmetry around the ray connecting the centers of the image, object, pupils, and vertices of the elements is broken because of the asymmetries in the free-form mirror, classifying this system as off axis. It is necessary to study the minimum fold angle to keep the incidence angles of the rays on the mirror as small as possible. In the case of a magnifier composed of the minimum number of optical elements, exploiting the degrees of freedom in free-form surfaces, such as the local anamorphisms, leads to compact off-axis magnifier designs like those presented in this paper. We are using the term "free-form" in reference to surfaces that are nonrotationally symmetric; examples of free-form surfaces include $x-y$ polynomials or Zernike polynomials. Recent advances in diamond turning technology facilitate the fabrication of non-rotationally-symmetric free-form surfaces.

A single $x-y$ polynomial surface mirror configured for an 8 mm exit pupil, 20° field of view, and 15 mm eye clearance, can only be tilted up to about 6° based on a modulation transfer function (MTF) metric. The polychromatic MTF drops below the desired 20% mark at the Nyquist frequency imposed by the microdisplay pixel spacing for tilt angles larger than 6°.

A dual-element solution needs to be considered to achieve a larger tilt angle. Adding a lens closer to the microdisplay improves the level of aberration correction of the field-dependent aberrations for the off-axis configuration. In our implementation, the lens closer to the microdisplay contains a diffractive optical element (DOE). An early feasibility study of the dual-element solution was presented at the International Optical Design Conference [4]. The new contributions in this paper include a full hardware implementation of the design for one eye, a demonstration of the imaging capability of the optics, and an analysis of the DOE. The optical layout is shown in Fig. 1(a) and consists of an 8 mm exit pupil, a free-form mirror, a hybrid refractive–diffractive lens, a flat fold mirror and a transmissive microdisplay. The free-form mirror is tilted at 34° in the $x-z$ plane with respect to the optical axis of the human eye. We found this angle to be the minimum tilt angle that can provide the necessary clearances around a human head based on a database of publicly available CAD models of human heads [5]. Typically, in a head-worn display the pupil of the human eye is the aperture stop of the system; therefore the aperture stop and the exit pupil coincide in this system. Even though magnifiers do not form exit pupils, it is customary to optimize these systems across a finite pupil size that is larger than that of the human eye to accommodate natural eye movements. Since under photopic illumination the pupil of the human eye is about 3 mm, it is customary to conduct the analysis for a 3 mm eye pupil for both centered and decentered pupils. The polychromatic MTF evaluated for a centered 3 mm pupil is plotted in Fig. 1(b) for the on-axis field and the performance-limiting fields. The MTF across decen-

 

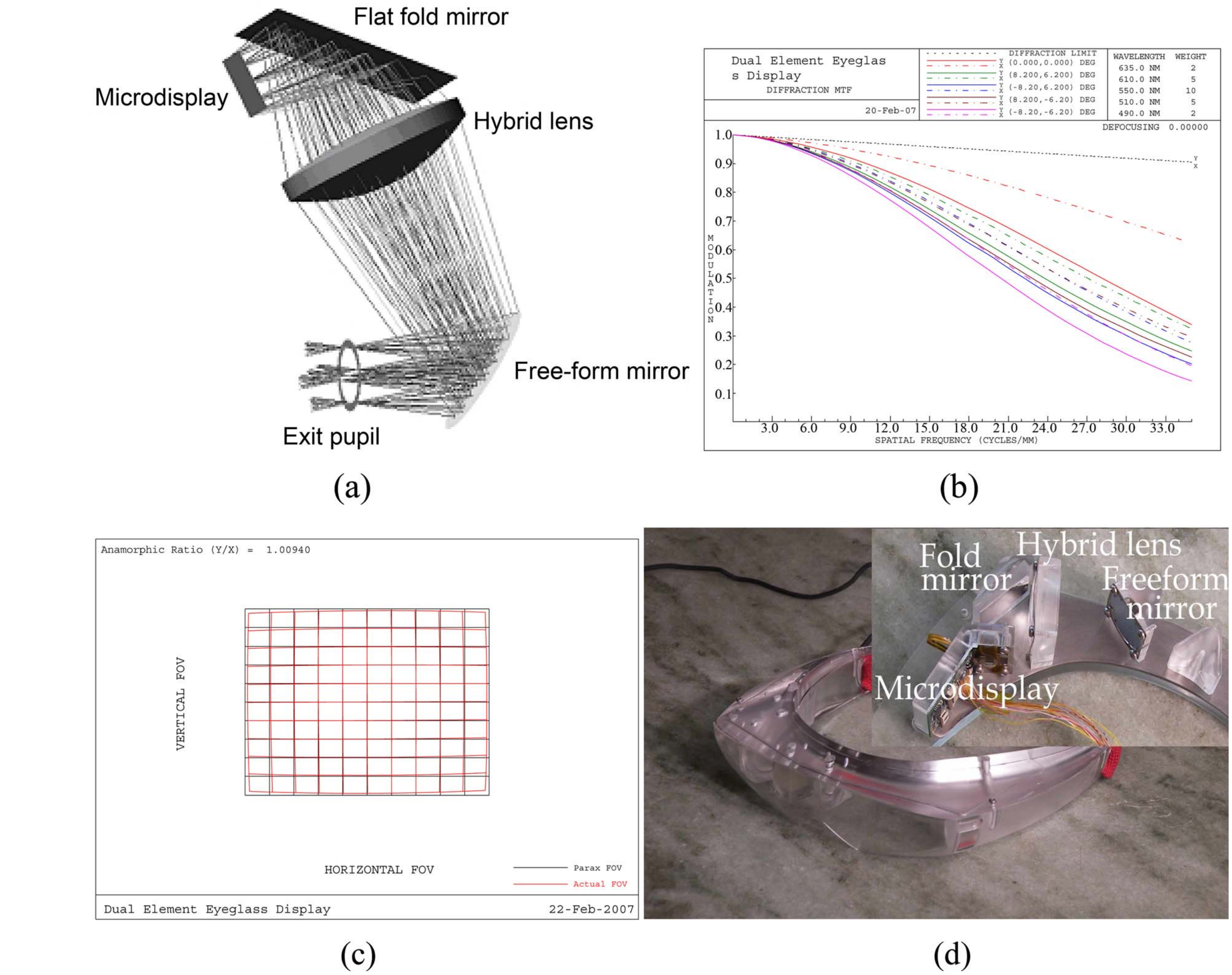


Fig. 1. (Color online) (a) Optical layout and the MTF of the near-eye magnifier. (b) MTF of the dual-element solution evaluated with a 3 mm pupil. (c) Distortion grid comparing real and paraxial rays. (d) Photograph of the fabricated and assembled near-eye magnifier.

tered pupils up to 6 mm in various directions displayed a performance similar to the centered pupil MTF. A red, blue, and green microdisplay pixel triplet is 14.1 $\mu$m in size, which yields a Nyquist frequency of 35 cycles/mm. Thus the polychromatic MTF was plotted up to 35 cycles/mm. In the current prototype, the microdisplay has a 0.44 in. diagonal and contains $640\times 480$ pixels. In visual space, the display provides 1.5 arcmin of resolution as limited by the pixel spacing on the microdisplay. It may be noted that a calculation of the Nyquist frequency given a 2.5 $\mu$m cone spacing of the human visual system yields a 1 arcmin resolution limit for the human visual system. The magnitude of maximum distortion occurs at ($x=8.2°$, $y=-6.2°$) in the field and was measured in simulation to be −3.8%. Figure 1(c) shows a plot of the real rays compared with the paraxial rays.

The optimization strategy was based on imposing the absolute minimum number of constraints on the system. Specifically, we optimized with the focal length, eye clearance and ray-based distortion constraints, since these form the minimum set of constraints. The focal length was constrained to a target value of 32 mm. The eye clearance was constrained to equal 20 mm. Optimization variables included the spacings between the elements and the surface coefficients.

To assess manufacturability, the sag range on the free-form mirror at 23 mm, at the edge of the mirror where maximum sag occurs, was computed to be 80 $\mu$m from the best-fit sphere. We used a 3 mm thick PMMAO material as the substrate for the free-form polynomial mirror. Plastic was selected because plastics are lighter in weight than typical glasses. The profile of the fabricated $x-y$ polynomial surface was described by the following polynomial:

$$P(x,y)=\frac{cr^2}{1+\sqrt{1-(1+k)c^2r^2}}+\sum_{j=2}^{10}C_jx^my^n,$$
$$j=\frac{(m+n)^2+m+3n}{2}+1, \qquad (1)$$

where $c$ is the vertex curvature, $r^2$ equal $x^2+y^2$, $k$ is the conic constant, and $C_j$ are the coefficients of the various $x^my^n$ terms. This surface was fabricated with a Moore 350 UPL with $c$ axis (slow slide servo).

The lens consists of a spherical surface and an aspheric surface with a DOE. It was found that the aspheric substrate improved the level of aberration cor-

(a)

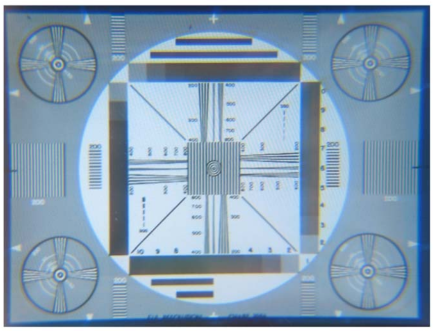

(b)

Fig. 2. (Color online) Photograph through the fabricated dual-element system of (a) a color target and (b) a black and white target.

rection. The lens was built out of Zeonex Z-ER48 material [6]. Diamond turning can produce the aspheric substrate along with the DOE at no additional cost. The DOE was configured to operate in the +1 diffracted order. The focal length of the DOE was given by $-0.5/c1$, where $c1$ is the quadratic phase coefficient of the DOE. In our case, the DOE contributes about 5% of the optical power on the plastic lens. The diffractive element can be viewed as a Fresnel zone plate. It is possible to use the focal length of a Fresnel zone plate, the Abbe number, and the relation for optical power to show that the Abbe value of a DOE in the visible is about −3.5 [7]. Therefore DOEs exhibit dispersion complementary to that of optical glasses and plastics, and they can be used in color correction. The profile of the hybrid lens was defined by an aspheric component whose coefficients were initialized to be zero and were allowed to vary during optimization.

The periodic grating structure of the DOE was defined by a phase function $\phi$, given by

$$\phi = \frac{2\pi}{\lambda}\sum_{i=1}^{4} c_i r^{2i},$$

where $\lambda_0$ is the design wavelength (558 nm in our design). Coefficients $c_i$ $(i=1\ldots4)$ were initialized to zero and were allowed to vary. The DOE and the aspheric surface were placed on the side toward the free-form mirror. The diffractive element was fabricated with 198 rings and a minimum feature size of 19 $\mu$m. The step height at the design wavelength of 558 nm is 1 $\mu$m. The radius of the DOE element is 28 mm. Diffraction efficiency at the wavelength of 550 nm is 98.7% and is above 90% across 490–635 nm for 16 mask levels in the case of a lithography-based process. The hybrid lens was fabricated by using diamond turning, and we can expect a diffraction efficiency equivalent to at least a 16 layer process, given that it is possible to fabricate 256-level DOEs by using diamond turning [8]. The hybrid lens was fabricated with a Precitech nanoform 350 two-axis diamond turning lathe. The distance between the center of the pupil and the vertex of the free-form mirror is 20 mm. The distance between the vertex of the free-form mirror and the vertex of the hybrid lens is 29.5 mm. The distance between the spherical surface of the hybrid lens and the fold mirror is 9 mm, and the distance between the fold mirror and the microdisplay is 14 mm. The axial color was extracted from the longitudinal spherical aberration plot and was measured to be approximately 20 $\mu$m. The maximum lateral color was measured to be 7.2 $\mu$m in the $(x=-8.2°, y=-6.2°)$ field. The detailed lens prescription, including the surface coefficients, is provided in a U.S. Patent application [9].

The assembled design is shown in Fig. 1(d). Color and black and white images formed by the dual-element off-axis magnifier are shown in Figs. 2(a) and 2(b). The whole assembly weighs approximately 250 g, including the outer shell, optics, optomechanical mounts, microdisplay, and the microdisplay driver electronics circuit board.

This work was supported in part by the Florida Photonics Center of Excellence and National Science Foundation grant IIS/HCI 03-07189. We thank Optical Research Associates for the educational license for CODE V, which was used for this research. We thank Adam Oranchak for designing the optomechanics.

## References

1. O. Cakmakci and J. Rolland, J. Disp. Technol. **2**, 199 (2006).
2. D. Bettinger, “Spectacle-based display system,” U.S. Patent 4,806,011 (February 21, 1989).
3. I. Kasai, Y. Tanijiri, T. Endo, and H. Ueda, *Fourth International Symposium on Wearable Computers (ISWC’00)* (IEEE Computer Society, 2000), pp. 115–118.
4. O. Cakmakci, A. Oranchak, and J. Rolland, Proc. SPIE **6342**, 63420W (2006).
5. Computerized Anthropometric Research and Design Laboratory, Warfighter Interface Division, Human Effectiveness Directorate, Air Force Research Laboratories, “CARD Database” (February 19, 2007) http://www.hec.afrl.af.mil/HECP/Card4.shtml.
6. Zeon Corporation (February 19, 2007) http://www.zeon.co.jp/index_e.html.
7. T. Stone and N. George, Appl. Opt. **27**, 2960 (1998).
8. L. Li, A. Y. Yi, C. Huang, D. A. Grewell, A. Benatar, and Y. Chen, Opt. Eng. **45**, 113401 (2006).
9. O. Cakmakci and J. P. Rolland, “Imaging systems for eyeglass based display devices,” U.S. patent application 11/398277 filed February 2006.